Supplemental Figures

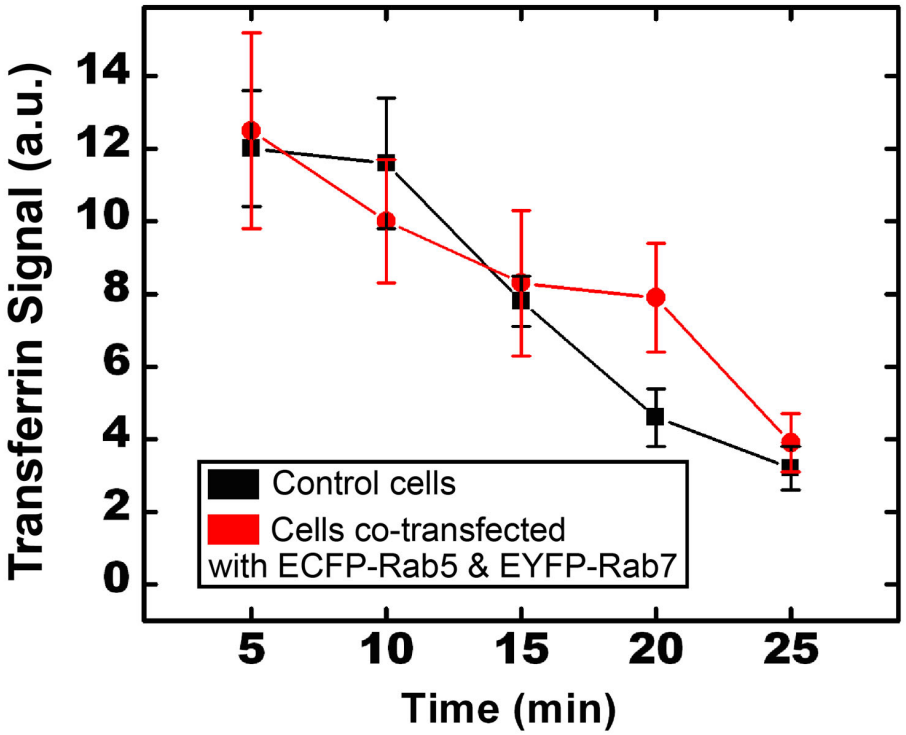

Figure S1: The expression of ECFP-Rab5 and EYFP-Rab7 does not significantly affect the recycling kinetics of transferrin.
The overall fluorescence signal from Alexa 647-labeled transferrin per unit area of the cells is plotted as a function of time for untransfected cells (black) and cells co-transfected with EYFP-Rab7 and ECFP-Rab5 (red). The decay of fluorescence is due to recycling and subsequent loss of transferrin into the surrounding medium. Experimental procedure: Untransfected or transfected BS-C-1 cells were incubated with Alexa 647-labeled transferrin at 0^{o}C. Unbound transferrin was washed away and the temperature was raised to 37˚ C rapidly to allow endocytosis and recycling for 5, 10, 15, 20 and 25 min. Cells were then fixed on ice and imaged.

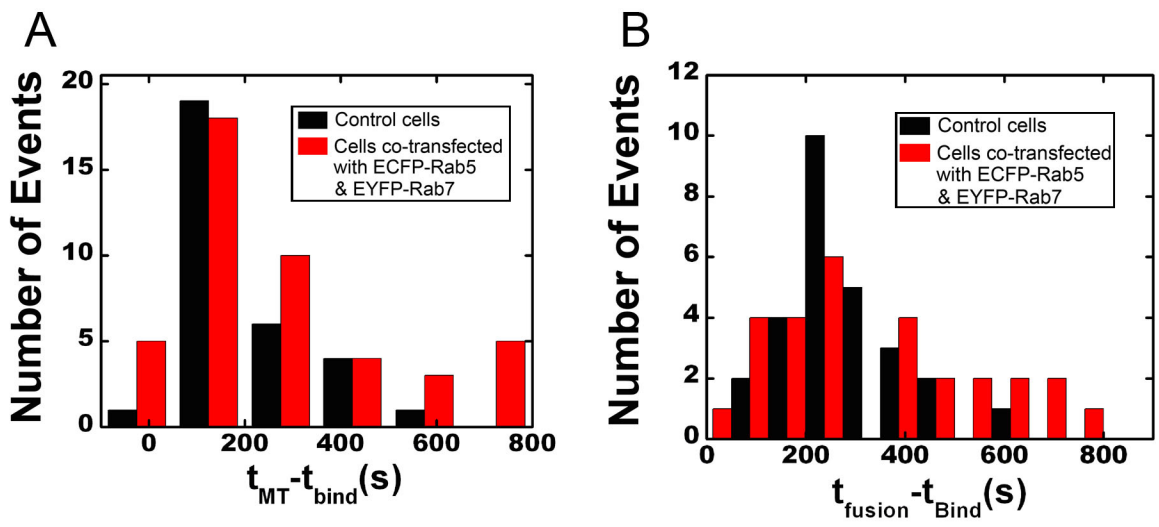

Figure S2: The expression of ECFP-Rab5 and EYFP-Rab7 does not significantly affect the internalization and fusion kinetics of influenza viruses.
(A) According to our previous work, influenza virus particles undergo rapid, microtubule-dependent transport from the cell periphery towards the perinuclear region. This microtubule-dependent transport quickly follows uncoating of the clathrin-coated vesicle carrying the virus (Lakadamyali et al., 2003; Rust et al., 2004). Here we use the onset of this microtubule-dependent transport as an indication for internalization and determine the time that it takes for each virus particle to begin microtubule-dependent motion after binding to the cell surface (t_{MT} - t_{bind}). Plotted are histograms of t_{MT} - t_{bind} for many randomly selected virus particles in untransfected BS-C-1cells (black) and cells co-transfected with EYFP-Rab7 and ECFP-Rab5 (red). The viruses were labeled with DiD and added to cells *in situ* at 37^{o}C.
(B) The lipid bilayer of the virus must fuse with an acidic endosome before the viral genetic material can be delivered into the cytoplasm. Here we determine the time that it takes for each virus particle to fuse with an endosome after binding to the cell surface (t_{fusion} - t_{bind}). Fusion events are identified by fluorescence dequenching caused by the spreading of DiD into the much larger endosome membrane (Lakadamyali et al., 2003). Plotted are fusion time histograms for many randomly selected virus particles.

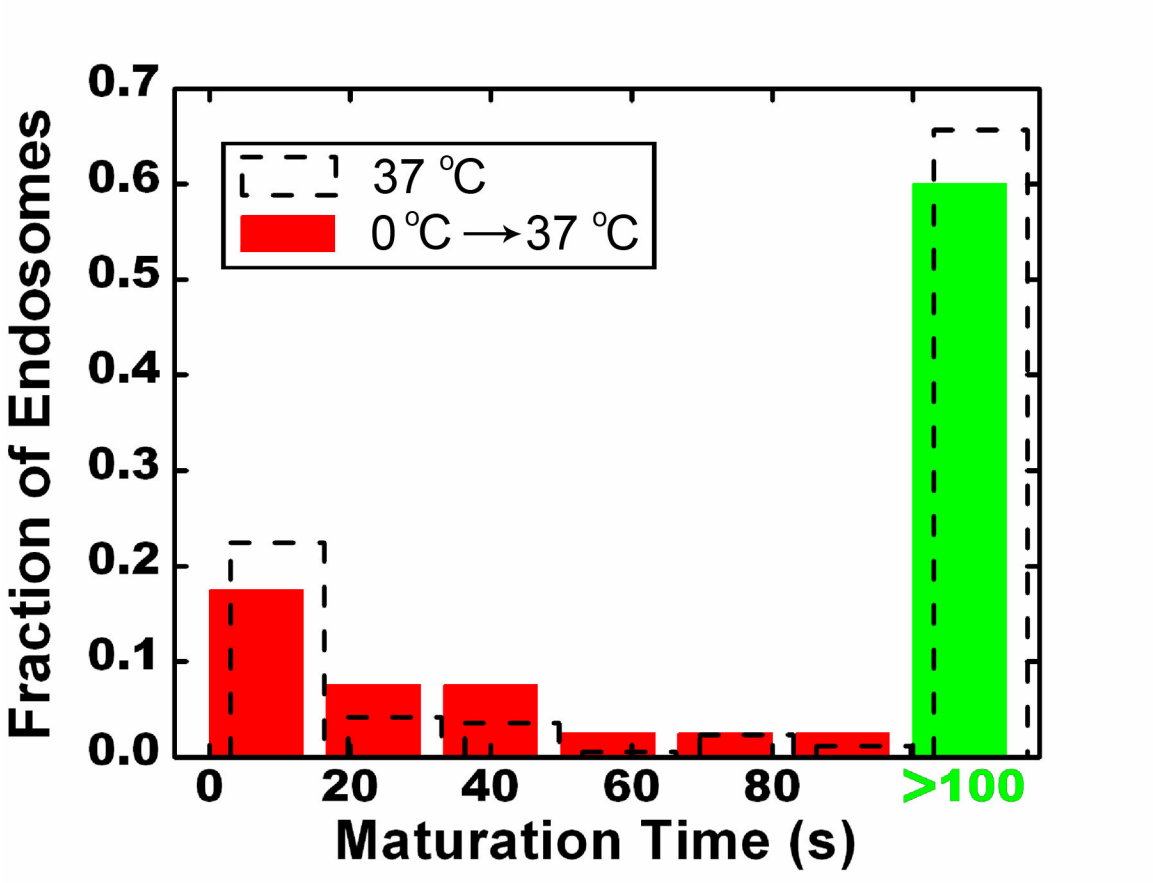

Figure S3: Temperature jump does not affect the endosome maturation kinetics.
Cells co-transfected with ECFP-Rab5 and EYFP-Rab7 were incubated on ice for 15 minutes, transferred to the microscope stage and warmed to 37 ^{o}C using a temperature-controlled microscope stage. Data was taken three minutes after the temperature jump. The maturation time histogram obtained in these cells (color columns) agrees well with that obtained in cells that have always been kept at 37 ^{o}C (dashed columns).

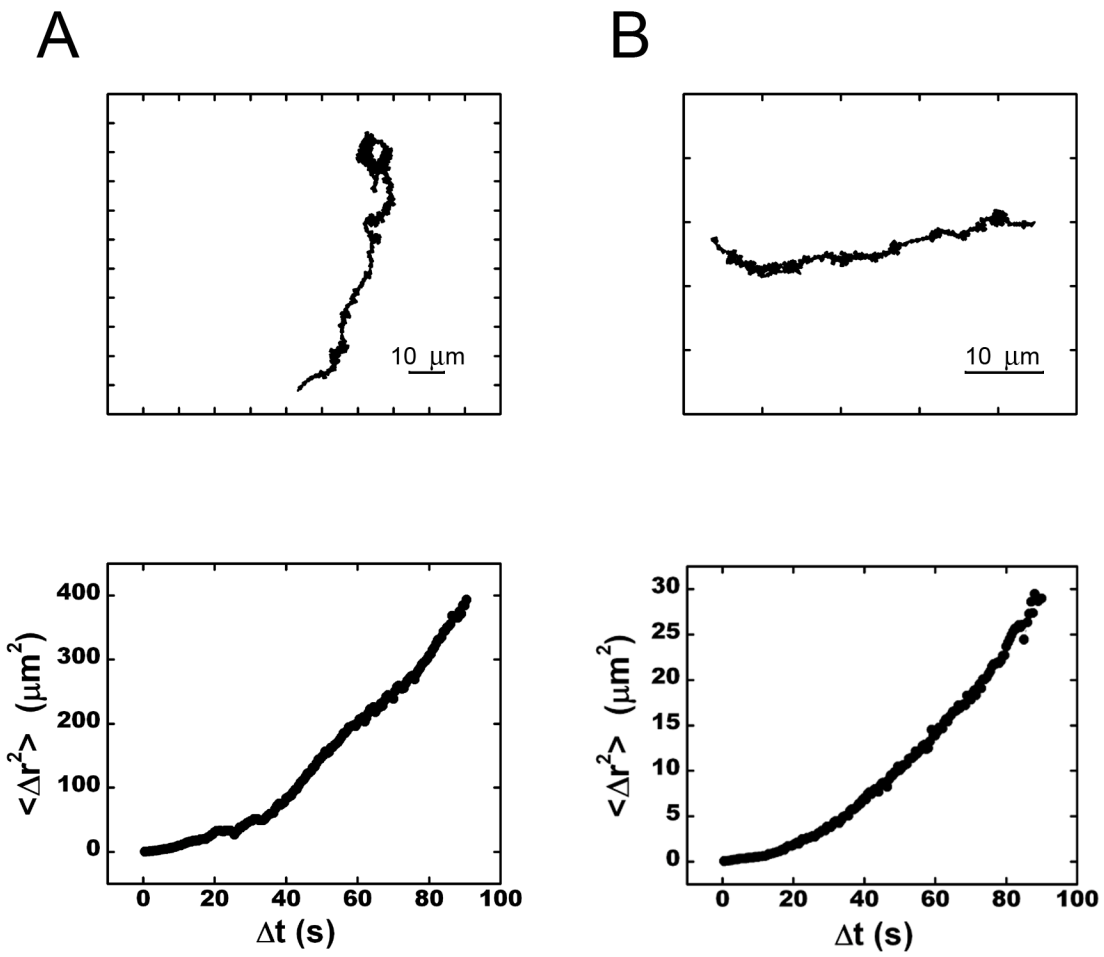

Figure S4. Physical trajectory (top) and mean-square-displacement versus time (bottom) for two exemplary dynamic endosomes (A and B). As endosomes exhibit intermittent rapid and directed transport separated by pauses during which the endosomes undergo slow and seemingly random movement that is probably due to diffusion, we screened for the periods of rapid transport with instantaneous velocity greater than 0.25 μm/s. The total lengths of the trajectories sampled are typically longer than 150 frames (75 s). The mean-square-displacement, $\langle \Delta r^2 \rangle$, is calculated for these periods. The $\langle \Delta r^2 \rangle$ vs. Δt is clearly super-linear indicating active transport.

A

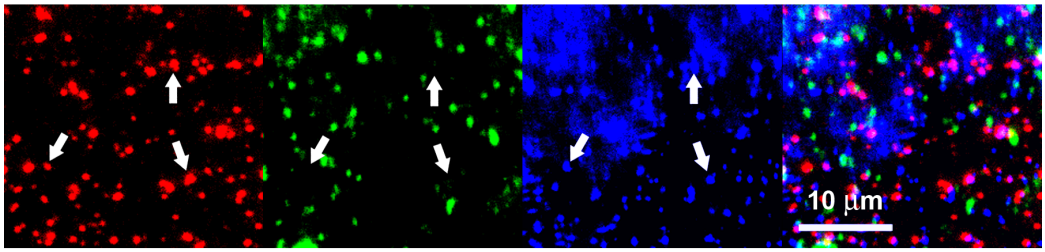
10 μm
Tfn
EYFP-Rab7
ECFP-Rab5
MERGE

B

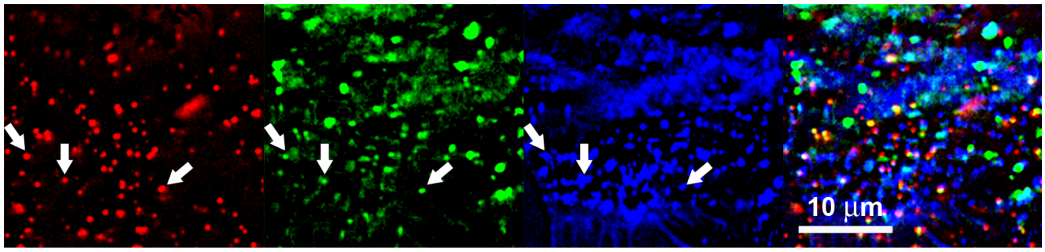
10 μm
LDL
EYFP-Rab7
ECFP-Rab5
MERGE

C

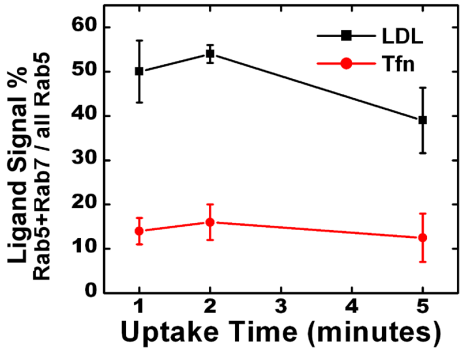
Ligand Signal %
Rab5+Rab7 / all Rab5
LDL
Tfn
Uptake Time (minutes)

D

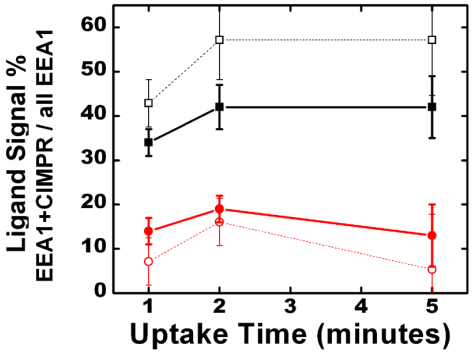
Ligand Signal %
EEA1+CIMPR / all EEA1
Uptake Time (minutes)

E

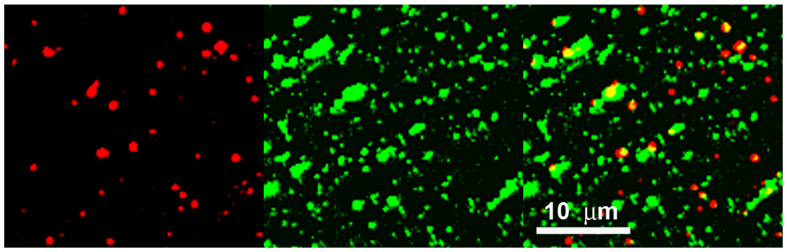
10 μm
LDL
Tfn
MERGE

Figure S5. Global analysis of the transferrin and LDL distribution in endosomes. In these experiments, ligands (transferrin (Tfn) or LDL) were added to cells for various amounts of time at 37^{o}C before fixation and their colocalization with Rab5, Rab7, EEA1 and CI-MPR proteins was analyzed in the fixed cells.

(A) Alexa 647-labeled transferrin (50 μg/mL) was added to cells co-expressing ECFP-Rab5 and EYFP-Rab7 at 37 ^{o}C. After 2 minutes, cells were washed with ice cold medium and fixed. Shown are fluorescence images for transferrin (red), EYFP-Rab7 (green), ECFP-Rab5 (blue) and a three-color composite. Most transferrin molecules that entered Rab5-positive endosomes do not colocalize with Rab7 (three examples are indicated by arrows).

(B) DiD-labeled LDL (20 μg/mL) was added to cells co-expressing ECFP-Rab5 and EYFP-Rab7 at 37 ^{o}C. After 2 minutes, cells were washed with ice cold medium containing heparin and fixed. LDL particles in Rab5-positive endosomes show a large degree of colocalization with Rab7. Arrows mark examples of LDL spots that colocalize with both Rab5 and Rab7. We note that some of the non-internalized LDL still remains on the cell surface after heparin treatment, and separate experiments using acid wash further reduce the surface density of uninternalized LDL particles.

(C) Quantitative analysis of the colocalization of LDL (black) and transferrin (red) with Rab proteins after adding these ligands to the cells for 1, 2, and 5 min. Plotted is the ratio between the total amount of ligand (transferrin or LDL) present in Rab5 and Rab7 co-positive endosomes and the total ligand signal in all Rab5-positive endosomes. These observations are quantitatively consistent with the single-particle tracking results, which show that transferrin is non-selectively delivered to all Rab5 endosomes, among which only 14% contain Rab7, whereas LDL particles are preferentially delivered to the rapidly maturing endosomes with 53% of LDL being delivered directly to endosomes containing both Rab5 and Rab7.

(D) To test whether this differential sorting behavior for LDL and transferrin may be potentially caused by the expression of ECFP-Rab5 and EYFP-Rab7, the global distributions of transferrin and LDL (Cy5-labeled) were also analyzed in non-transfected cells. After adding ligands to the cells for 1, 2, and 5 min, cells were fixed and stained for immunofluorescence against EEA1 and CI-MPR. Plotted is the ratio between the total amount of ligand in EEA1 and CI-MPR co-positive endosomes and the total ligand signal in all EEA1-positive endosomes (solid symbols). This ratio is low for transferrin but starts out much higher for LDL. Considering that 10% of Rab5-only endosomes and 57% of Rab5 and Rab7 co-positive endosomes colocalize with CI-MPR, we estimated the fraction of ligands in Rab5 and Rab7 co-positive endosomes by taking these factors into account (open symbols). This estimate agrees quantitatively with the results obtained in ECFP-Rab5 and EYFP-Rab7 expressing cells (shown in (C)), indicating that the expression of fluorescent Rab proteins did not alter the trafficking behavior significantly.

(E) DiD-LDL (20 μg/mL) and TMR-transferrin (50 μg/mL) were added to cells simultaneously at 37 ^{o}C for 2 minutes. Cells were washed in ice-cold acidic buffer to remove most of the surface-bound material then chased for 3 minutes at 37 ^{o}C, fixed and imaged. Although LDL-positive spots (red) substantially overlap with transferrin (green), the converse is not true. This is consistent with transferrin being indiscriminately delivered to all early endosomes, while LDL is preferentially targeted to a subset of the early endosomes.

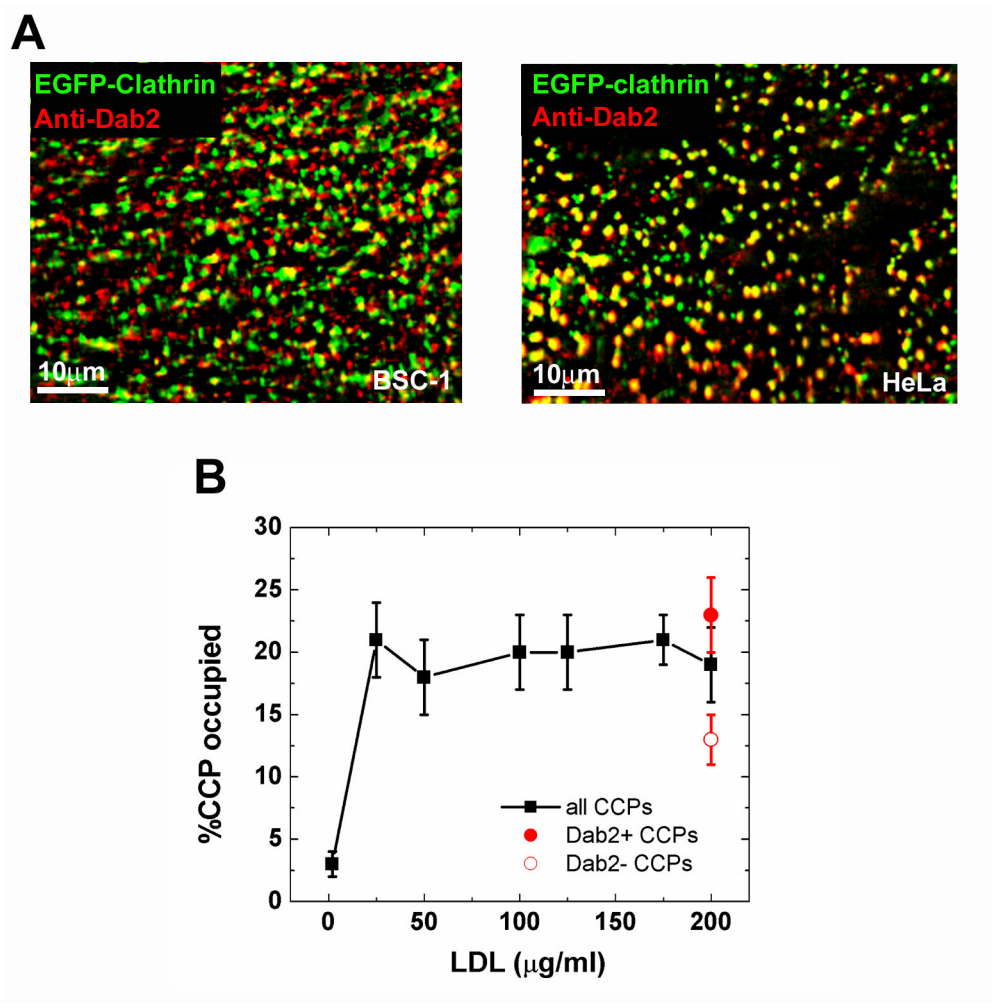

Figure S6: Colocalization between Dab2 and CCPs and the preferential association of LDL with Dab2-positive CCPs.

(A) Colocalization between clathrin and Dab2. EGFP-clathrin expressing BSC-1 and HeLa cells were saponin-extracted, fixed and immunostained for Dab2. In BSC-1 cells, roughly 30% of CCPs show colocalization with Dab2 spots. A computer simulation with the same density and size of Dab2 spots shows that less than 8% of CCPs would colocalize with Dab2 if Dab2 does not preferentially associate with CCPs, but distributes randomly. In HeLa cells, roughly 60% of CCPs show colocalization with Dab2, which agrees quantitatively with previous results (Morris and Cooper, 2001).

(B) Fraction of CCPs occupied by LDL in HeLa cells. After incubation of EGFP-clathrin expressing HeLa cells with LDL for 3 min at 37^{o}C, cells were saponin-extracted, fixed and imaged. No matter how high a concentration of LDL was used, the fraction of CCPs loaded with LDL saturated at about 20%. Immunostaining for Dab2 further shows that the fraction of Dab2-positive CCPs occupied by LDL is about 2-fold larger than the fraction of Dab2-negative CCPs occupied by LDL, similar to the results obtained in BSC-1 cells.

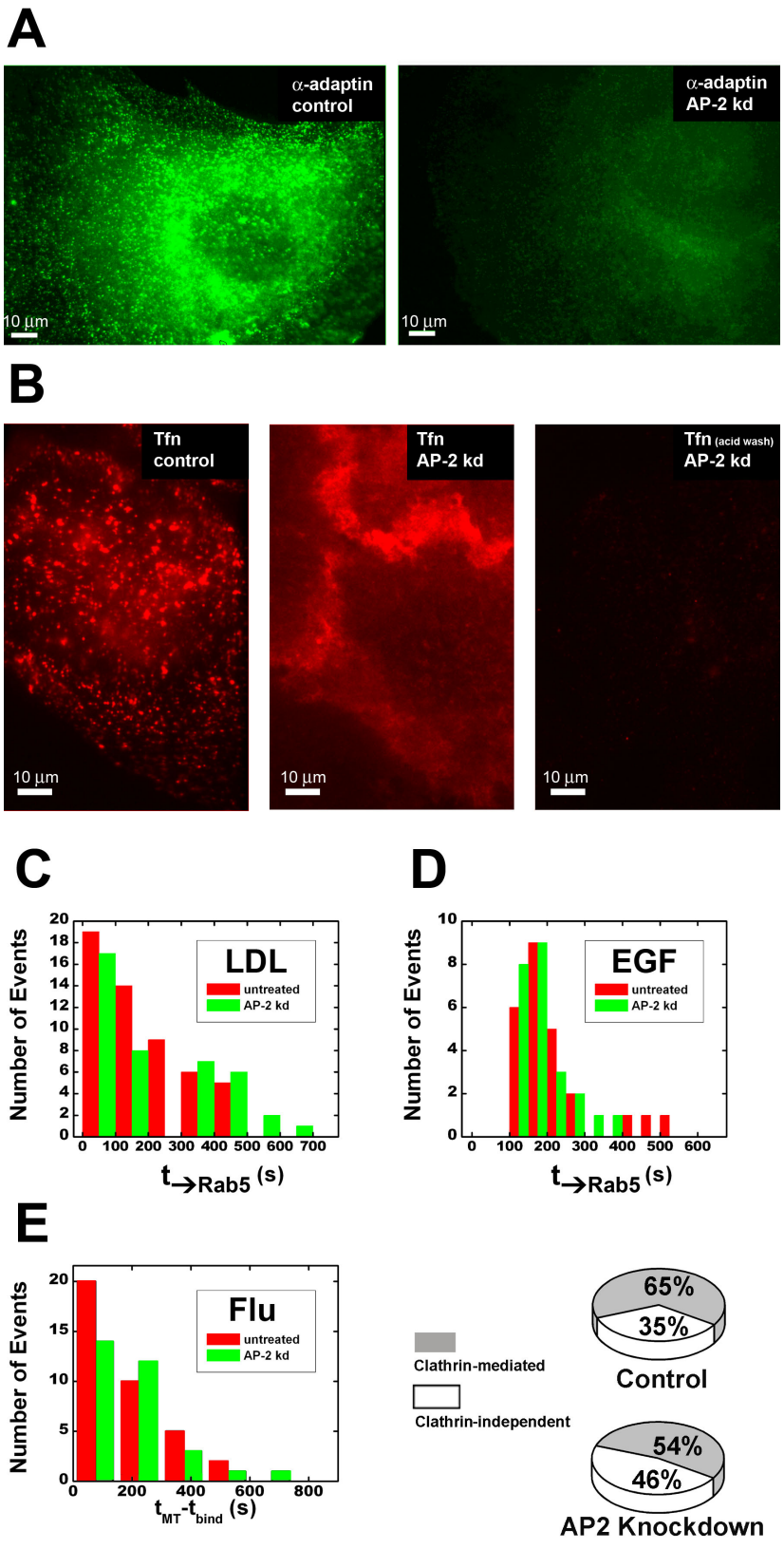
A
α-adaptin control
α-adaptin AP-2 kd
10 µm
10 µm
B
Tfn control
Tfn AP-2 kd
Tfn (acid wash) AP-2 kd
10 µm
10 µm
10 µm
C
LDL
untreated
AP-2 kd
Number of Events
t→Rab5 (s)
D
EGF
untreated
AP-2 kd
Number of Events
t→Rab5 (s)
E
Flu
untreated
AP-2 kd
Number of Events
t_MT-t_bind (s)
Clathrin-mediated
Clathrin-independent
65%
35%
Control
54%
46%
AP2 Knockdown

Figure S7. Effect of AP-2 knockdown on the uptake of transferrin, LDL, EGF, and influenza virus.

(A) Immunofluorescence against the α-subunit of AP-2 in control cells and in cells treated with siRNA to knockdown AP-2. Both images were taken under identical laser excitation conditions. Consistent with previous work (Motley et al., 2003), the expression of α-subunit is much reduced and shows very dim spots at a lower density compared to untreated cells. Reduction in the expression of the μ2-subunit of AP-2 was also confirmed by Western blot (not shown).

(B) Transferrin uptake is blocked by AP-2 knockdown. Alexa 647-labeled transferrin (50 μg/mL) was bound to control cells (left) or AP-2 knockdown cells (middle and right) on ice. Unbound ligand was removed, and endocytosis was allowed to proceed at 37 ^{o}C for 5 minutes. In the right panel, surface-bound, uninternalized transferrin was removed using an acidic buffer (0.2M acetic acid, 0.5M sodium chloride). Cells were then fixed and imaged using identical imaging conditions. Unlike in untreated cells, no detectable signal of transferrin is found in punctate endosomes in AP-2 knockdown cells, and upon removal of the surface-bound transferrin, little transferrin signal is left in the cells, indicating that the transferrin uptake is blocked by AP-2 knockdown.

(C) LDL entry is not inhibited by AP-2 knockdown. The total amount of LDL that reached Rab5-positive endosomes is identical within 11% for control and AP-2 knockdown cells. We further quantified the uptake rate of LDL by measuring the time it takes each LDL particle to reach a Rab5-positive endosome after the temperature was raised to 37 ^{o}C. Plotted are the time histograms from many randomly selected LDL particles in control (red) and AP-2 knockdown cells (green). No statistically significant difference was found between the two cases.

(D) EGF entry is not inhibited by AP-2 knockdown. Analysis is similar to (C). The total amount of EGF that reached Rab5-positive endosomes is identical within 6% for control and AP-2 knockdown cells. There is also no statistically significant difference in the uptake rate.

(E) Influenza entry is not affected by AP-2 knockdown. (Left panel) The histogram of internalization time for influenza viruses in control (red) and AP-2 knockdown cells (green). The internalization time of a virus particle is defined as the time between binding to cell (t_{bind}) and the onset of microtubule dependent movement (t_{MT}), which quickly follows clathrin uncoating, as we have shown previously (Rust et al., 2004). The internalization rates of influenza in control and AP-2 knockdown cells are identical within error. (Right panel) The fractions of virus particles that are internalized by the clathrin-mediated or clathrin-independent endocytic pathways in control and AP-2 knockdown cells. The difference between the two cases is not statistically significant.

Supplemental experimental procedures

Cell Culture

BS-C-1 cells were maintained in a 5% CO_2 environment at 37 °C in MEM with 10% (v/v) FBS unless otherwise mentioned. In some cases, cells were incubated with the lipoprotein-deficient serum overnight before experiments, as specified in the text.

Transfection

We transiently transfected BS-C-1 cells with fluorescent protein constructs 24 hours after the cells were plated. Solutions containing 1-2 μg of plasmids and 6-9 μL of FuGENE 6 in 100 μL of MEM was used for transfection. Experiments were conducted either 24 or 48 hours post-transfection.

Immunofluorescence

Cells were fixed in 2% (v/v) formaldehyde for 40 min. After being washed in PBS, the cells were permeabilized in a blocking buffer containing 10% (v/v) FBS, 3% (w/v) BSA and 0.5% (v/v) Triton X-100 in PBS. The cells were then incubated at 4 °C with primary antibodies against EEA1, CI-MPR, clathrin heavy chain or the α subunit of AP-2 for 6-12 hours. Excess antibody was removed by extensive washing with PBS containing 0.2% (w/v) BSA and 0.1% (v/v) Triton X-100, and the cells were then incubated at room temperature for 30 min with secondary antibodies (Molecular Probes). For immunofluorescence experiments involving transferrin, experimental procedures are similar except that the blocking buffer used contains 0.1% Tween 20 and 5% BSA and the wash buffer contains 0.1% Tween 20 and 1% BSA. For immunofluorescence against Dab2, cells were extracted with 0.03% saponin in cytosolic buffer (25mM Hepes, pH 7.4, 25 mM KCl, 2.5 mM magnesium acetate, 5 mM EGTA and 150 mM K-glutamate) for 1 min prior to fixation with 4% paraformaldhyde for 20 min. These cells were then permeabilized in 0.1% Triton X-100 for 10 min, blocked in PBS containing 1%BSA for 60 min, and then incubated with primary antibodies for 90 min and the appropriate secondary antibodies for 60 min.

AP2 knockdown by siRNA

To deplete cells of functional AP-2, BS-C-1 cells were transfected twice with siRNA against the μ2 subunit of AP-2, following a previously established protocol (Motley et al., 2003). Briefly**,** 50 μL of 20 μM siRNA solution was diluted to a total volume of 1 mL with 50 μL oligofectAMINE (Invitrogen) in serum-free OptiMEM (Invitrogen)**.** This mixture was added to cell culture in a total of 5 mL of OptiMEM. After 4 hours, 5 mL of MEM supplemented with 20% FBS was added to the cells. This knockdown procedure was performed twice, 24 hours apart, before cells were harvested or used for fluorescence experiments. The AP-2 expression level was tested by western blot against μ2 subunit and immunofluorescence against the α subunit.

Image analysis

Image analysis and single-particle tracking were carried out using custom-written software as previously described (Rust et al., 2004). Colocalization between different structures is identified by an automated program and confirmed by eye. As endosomes have mosaic structures, containing different domains enriched in different proteins, the criteria for colocalization is that the different colored objects (1) show at least partial overlap and (2) move together. In fixed cells, the second criterion cannot be used. To estimate the error in the calculated colocalization fraction due overlap by random chance, randomly distributed spots of two different colors with the same densities and spot sizes as in the experimental images were generated by simulation. This typically results a colocalization fraction smaller than 5%.

References:

Lakadamyali, M., Rust, M. J., Babcock, H. P., and Zhuang, X. (2003). Visualizing infection of individual influenza viruses. Proc Natl Acad Sci, USA *100*, 9280-9285.
Morris, S. M., and Cooper, J. A. (2001). Disabled-2 colocalizes with LDLR in clathrin-coated pits and interacts with AP-2. Traffic *2*, 111-123.
Motley, A., Bright, N. A., Seaman, M. N. J., and Robinson, M. S. (2003). Clathrin-mediated endocytosis in AP-2-depleted cells. J Cell Biol *162*, 909-918.
Rust, M. J., Lakadamyali, M., Zhang, F., and Zhuang, X. (2004). Assembly of endocytic machinery around individual influenza viruses during viral entry. Nat Struct Mol Biol *11*, 567-573.